Available online at www.sciencedirect.com
ScienceDirect
Applied Surface Science 253 (2006) 90–94
applied surface science
www.elsevier.com/locate/apsusc

Photoreflectance spectroscopy of self-organized InAs/InP(0 0 1) quantum sticks emitting at 1.55 μm

H. Chouaib [a,*], N. Chauvin [a], C. Bru-Chevallier [a], C. Monat [b], P. Regreny [b], M. Gendry [b]

[a] *Laboratoire de Physique de la Matière, INSA de Lyon (UMR-CNRS 5511), Bâtiment Blaise Pascal,*
7 Avenue J. Capelle, 69621 Villeurbanne, France
[b] *Laboratoire d'Electronique, Optoélectronique et Microsystèmes (UMR CNRS 5512), Ecole Centrale de Lyon,*
36 Avenue Guy de Collongue, 69134 Ecully, France

Abstract

Photoreflectance (PR) measurements are performed as a function of temperature on self-organized InAs/InP(0 0 1) quantum sticks (QSs) grown by solid-source molecular beam epitaxy. With a very weak excitation power, three PR transition energies are arising and associated with the ground state and two excited states, respectively, in good agreement with both photoluminescence (PL) and PL excitation measurements. The temperature dependence of the PR transition energies is in good agreement with the Bose–Einstein behavior.

From PL analysis of these InAs/InP QSs, the ground state was assumed to be partially filled because of the residual n-type doping of the InP barrier layers. The PR spectra analysis allows us to further confirm this assumption, considering mainly the relative PR intensity of the different transitions, as well as the Franz Keldysh oscillations (FKO) above the InP bandgap.

Keywords: Photoreflectance spectroscopy; Quantum sticks; Photoluminescence; molecular beam

1. Introduction

The classical techniques to investigate the optical properties of nanostructures like quantum dots are photoluminescence (PL) [1], photoluminescence excitation (PLE) [2], time-resolved photoluminescence [3] and photocurrent spectroscopy [4]. PL is the principal useful technique due to its relative simplicity. However, only luminescence states are studied and the extracted information from PL are limited. Hence, in confined systems, a complementary technique like photoreflectance (PR) [5] spectroscopy is very useful to determine the energies of every direct optical transitions, their broadening parameters [6] and the oscillators strength [7], and eventually to measure the internal electric field value in n i p structures or at other space charge layers in the structure [8].

In this report, we use contactless PR in the temperature range 12–300 K to investigate the optical properties of InAs quantum sticks (QSs) grown by solid-source molecular beam epitaxy (MBE) on a semi-insulating InP(0 0 1) substrate. Many transitions are detected from InAs QSs and wetting layer (WL) and are identified by comparing with PL and PLE spectroscopy. The evolution of transition energy is studied versus temperature. The origin of Franz Keldysh oscillations (FKO) above InP gap is discussed.

2. Experiments

The self-organized InAs QSs are grown by solid-source MBE on a semi-insulating InP(0 0 1) substrate. A plane of InAs QSs embedded in InP barrier layers is grown with optimized growth parameters in order to reduce the stick size dispersion [9]. The InAs deposit thickness is adjusted to have an emission wavelength around 1.5 μm at room temperature. PL spectroscopy is performed at 12 K, using an Argon ion laser with a wavelength of 514.5 nm as the excitation source. The PLE is excited by a quartz–tungsten lamp dispersed through a 0.6-m double-grating spectrometer providing a tunable light source. The experimental PR setup is a conventional one [8]. The probe beam is provided from a tungsten halogen lamp dispersed through a grating monochromator and irradiated on the sample.

---

* Corresponding author.
E-mail address: houssam.chouaib@insa-lyon.fr (H. Chouaib).

0169-4332/$ – see front matter © 2006 Elsevier B.V. All rights reserved.
doi:10.1016/j.apsusc.2006.05.081

The modulated reflectance in QSs sample is produced by a mechanically chopped He–Ne laser beam at 320 Hz. The reflected light from the sample is focused on an InGaAs photodiode. The detected signal is amplified by a *I*/*V* converter. For the temperature dependent experiments, the samples are mounted in a cold finger variable temperature cryostat.

In PR experiments applied to confined systems, the pump beam intensity plays an important role. Indeed, the laser induced background PL parasitic signal is relatively significant at every temperature in such confined systems. In order to avoid masking the PR signal by the PL offset, the pump beam intensity is controlled by attenuator filters. The signal-to-noise ratio of PR spectra is shown to strongly depend on the pump–probe power ratio.

3. Results and discussion

The normalized PL spectra recorded at 12 K in the InAs QSs at different excitation power are shown in Fig. 1. A PL signal is detected between 0.82 and 0.94 eV. Except the low energy shoulder previously attributed to some defect influence [10], the PL spectra can be fitted using two gaussian lines. Two peaks (labeled A and B) are clearly resolved and are indicated by arrows at 0.870 and 0.905 eV, with full width at half maximum equal to 25 and 27 meV, respectively. In order to study the origin of these two peaks, we increase the laser power from 0.2 to 900 mW. The second peak B strongly increases as compared to the peak A. Therefore, we attribute the peak B to the first excited state related to the ground state (peak A). This behavior is explained by the fact that the ground state becomes saturated at high excitation power leading to the filling of the excited states [11]. The energy spacing between the ground state and the first excited state (35 meV) is in good agreement with the theoretical studies performed on similar samples [12].

It is interesting to note that the recombination from the excited state still remains at very weak excitation power, as previously reported [10]. Such a behavior has been tentatively attributed to the effect of non-intentional n type doping of the InP layers.

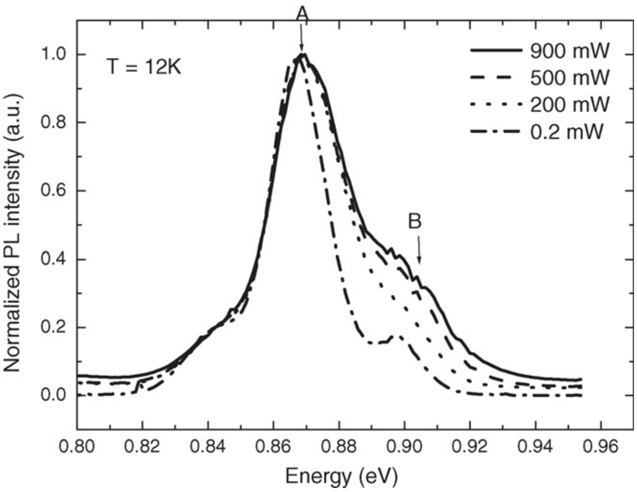

Fig. 1. PL spectrum recorded at 12 K in InAs/InP QSs, as a function of the excitation power.

The physical origin of the PL peaks was further confirmed from PLE spectroscopy [13], which allows the identification of confined states from both the QSs and the WL. The PLE spectrum at 12 K is shown in Fig. 2a, the detection energy being fixed at 0.870 eV. The spectrum clearly shows three absorption peaks labeled a, b and c at 0.908, 0.945 and 1.07 eV, respectively. The energy gap between *a* and *b* is roughly equal to that between ground state and first excited state. Then, we attribute peaks *a* and *b* to the first and second excited states, respectively, related to the ground state peak at 0.870 eV. The peak *c* in Fig. 2a is very broad, in the 1.02–1.152 eV energy range, and is attributed to the WL.

PR spectroscopy was applied to this sample in order to gain more information. The PR spectrum recorded at 12 K in the InAs QSs is shown in Fig. 2b. In the spectral range between 0.85 and 1.2 eV, four transitions are arising (labeled P1, P2, P3 and P4). Each of them was fitted using a Lorentzian lineshape [5]

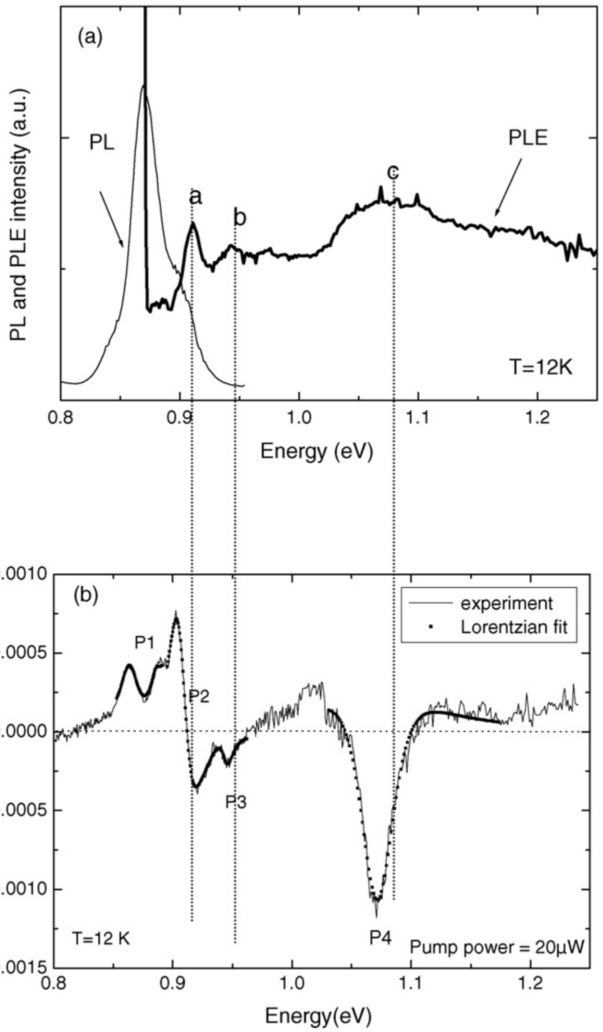

Fig. 2. (a) PL and PLE spectra recorded at 12 K in the InAs/InP QSs. The PLE energy detection is fixed at 0.870 eV. (b) PR spectrum recorded at 12 K in the same sample.

which can be expressed by:

$$\frac{\Delta R}{R} = Re(Ae^{i\phi}(E - E_n + i\Gamma)^{-2}) \qquad (1)$$

where A is the amplitude, ϕ the phase angle, E the photon energy, E_n the n transition energy, and Γ is the broadening parameter. The fitting lineshapes are plotted in Fig. 2b (dark squares).

A good agreement is obtained between PL, PLE and PR spectra as far as transition energies are concerned. The optical transitions observed are the ground state at 0.872 eV (P1) and two excited states (P2 and P3) at 0.909 and 0.945 eV, respectively. The WL signal is arising at 1.071 eV. The small energy shift between PL and PR transitions is attributed to Coulombic interactions. The PL peak energies are influenced by multiexciton effect. On the contrary, the PR spectrum is obtained at low excitation power (20 μW), which decreases the effect of Columbic interactions.

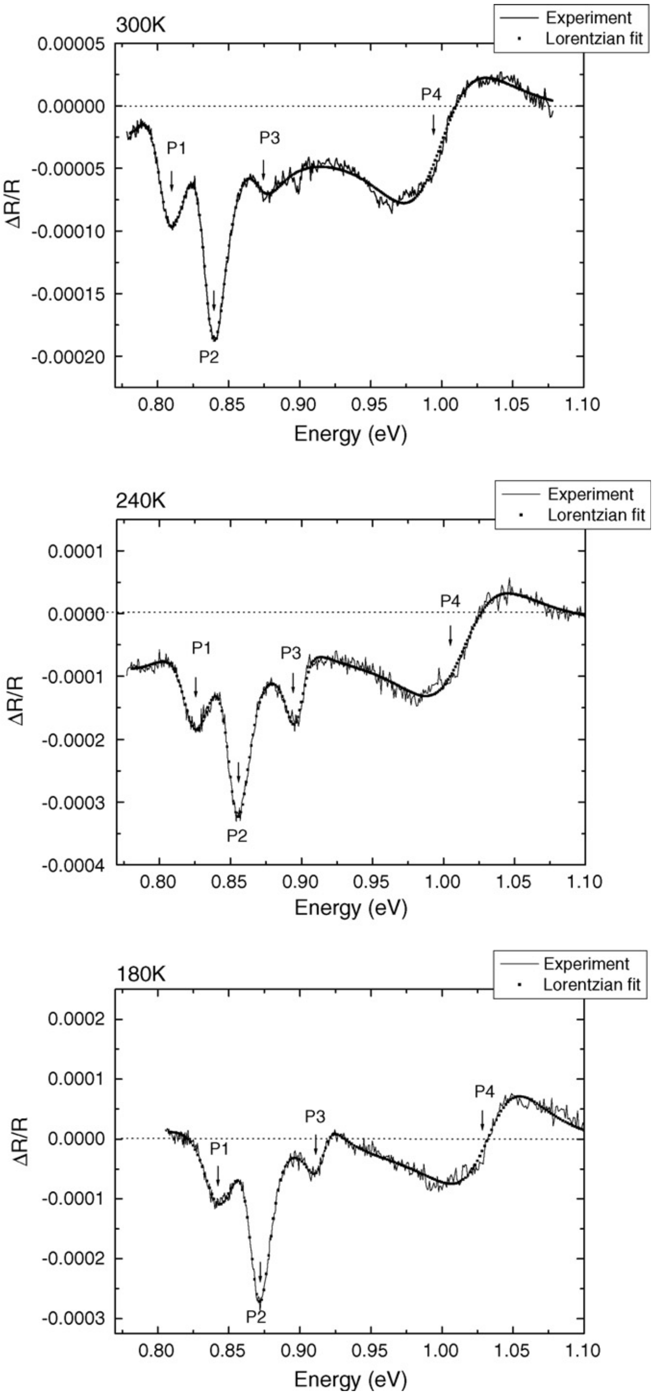

Fig. 3. PR spectra of InAs/InP QSs recorded at 300, 240 and 180 K.

Now, let us look at the PR intensity, which is proportional to the oscillator strength of the corresponding transition in confined systems [14]. A remarkable behavior appears by comparing the PR intensity of both transitions: ground state and first excited state. The ground state PR intensity is much lower than the first excited state one. We interpret this unusual behavior as a charging effect of QSs due to the effect of a non-intentional n doping of the InP layers. The ground state is assumed to be partially filled in this type of structures [10] and this weakens the absorption. Moreover, the electron charging in the QSs reduces the oscillator strength by separating the electron and hole wave functions. These two effects are responsible for the ground state PR intensity lowering.

The PR spectra recorded at different temperatures are plotted in Fig. 3. The transitions P1, P2, P3 and P4 are marked with arrows in the figure. The transition energies redshift as the temperature is increased. This evolution is fitted using the Bose–Einstein expression [15] given by:

$$E_G(T) = E_G(0) - \frac{2\lambda}{\exp(\theta/T) - 1} \qquad (2)$$

where λ is the average strength of the exciton–phonon interaction and θ is the average phonon temperature. The fitting curves are plotted in Fig. 4, and the parameter values derived from the fitting are listed in Table 1.

Among the parameters determined form fitting the PR transition using equation (1) is the broadening parameter Γ. Extracted values are 19, 16 and 19 meV at room temperature for the ground state, the first and second excited states, respectively.

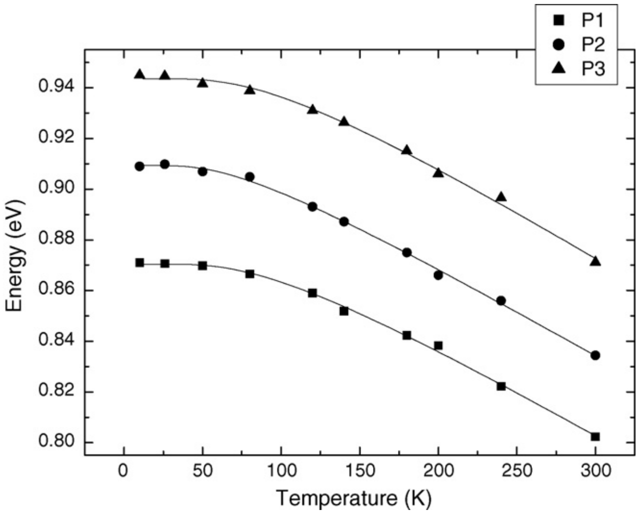

Fig. 4. Temperature dependence of the QSs transition energies (P1, P2 and P3). Solid lines are fits to the Bose–Einstein expression.

Table 1
Values of the Bose–Einstein fitting parameters for P1, P2 and P3 transitions

Transitions	$E_G(0)$ (eV)	λ (meV)	θ (K)
P1	0.871 ± 0.002	99 ± 12	270 ± 20
P2	0.909 ± 0.002	74 ± 9	206 ± 17
P3	0.944 ± 0.002	105 ± 17	275 ± 27

Table 2
Broadening parameter Γ at 300, 240, 180 and 12 K for P1, P2 and P3 transitions

Transition	300 K	240 K	180 K	12 K
P1 (meV)	19 ± 2	20 ± 2	24 ± 2	19 ± 2
P2 (meV)	16 ± 2	16 ± 2	16 ± 2	13 ± 2
P3 (meV)	19 ± 2	14 ± 2	13 ± 2	11 ± 2

Table 2 lists the broadening parameter values obtained at different temperatures. On the contrary to the expected behavior of the broadening parameter with temperature, no clear increase of Γ is observed for any of the transitions when temperature is increased. Γ (P1) is even slightly decreasing as temperature is increased from 180 and 300 K. In the case of a QD population, the broadening parameter Γ is mainly due to the distribution of the QD size, which is independent on the temperature. In a rather homogeneous QD population however, when Γ is lower than 20 meV, one would expect to observe the influence on Γ of increasing electron–phonon interaction as the temperature is increased. This we do not observe, as previously reported in literatures [6,16,17]. Further work is under way to understand in details the evolution of Γ as a function of temperature.

Finally, Fig. 5 shows the PR spectrum recorded at 200 K in the 1.3–1.4 eV energy range. Oscillations are observed above 1.3 eV and are tentatively attributed to Franz Keldysh oscillations (FKO) coming from a built-in electric field in the InP layers. The same kind of spectra with FKO is recorded in every studied sample. The FKO period is a direct measurement of the internal electric field. In order to determine the value of this electric field, we use the expression [8]:

$$E_m - E_G = \hbar\Omega\left(\frac{3}{4}(m\pi - \phi)\right)^{2/3} \qquad (3)$$

where m is the extremum index, $E_G = 1.382$ eV the InP energy gap at 200 K, E_m the PR extremum energy, Φ an arbitrary phase factor and $\hbar\Omega = (q^2F^2\hbar^2/2\mu)^{1/3}$ is the electro-optic energy with F the electric field, μ the reduced effective mass, and q and ħ being respectively the elementary charge and reduced Planck constant. Using $\mu = 0.067m_0$ for InP, we estimate the field value at about 6 kV/cm. We suppose that this small electric field could be caused by the charging of the QSs already highlighted above [10] and created by the non-intentional n doping of the InP layers. Following the work of Davydov et al. [18], the area surface charge density σ which could be responsible for this electric field is derived using the formula $\sigma = \varepsilon\varepsilon_0 F$ where $\varepsilon = 12.5$ is the InP dielectric constant. We find $\sigma = 3.6 \times 10^{10}$ cm^{-2} which is a reasonable value because the QS density was already estimated around 5×10^{10} cm^{-2} [19]. This is in good agreement with the fact that the QSs are partially filled by residual doping of the InP layer.

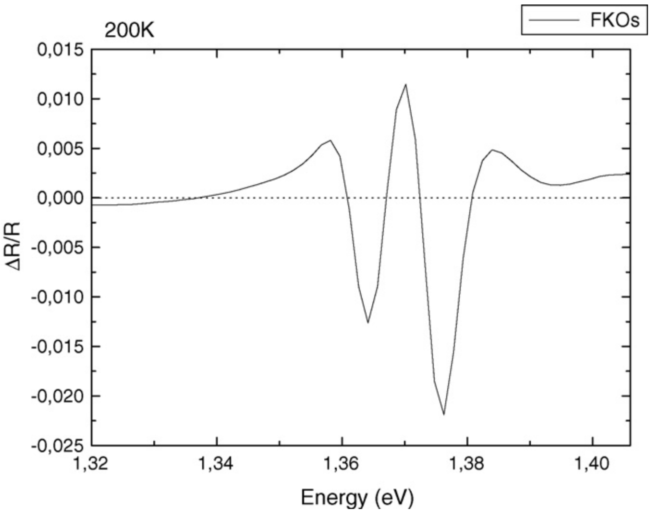

Fig. 5. PR spectrum of InAs/InP QSs recorded at 200 K in the 1.3–1.4 eV energy range.

4. Conclusion

In summary, optical properties of InAs/InP QSs are characterized by PR spectroscopy in the temperature range between 12 and 300 K. The PR experimental results are in good agreement with PL and PLE results. The great sensitivity of the PR technique is highlighted as compared to the PL technique for the QSs characterization. Energy positions of the ground state and the two excited states in the QSs are measured as well as one transition arising from the WL. The temperature dependence of the QS transition energies are fitted using Bose–Einstein expressions, and the broadening parameter Γ do not hardly show any variation versus temperature. We also detected the presence of a small electric field in the InP layer, which is tentatively attributed to the effect of the residual n-type doping of the InP layer, leading to electron charging of the QSs.

References

[1] S. Fafard, R. Leon, D. Leonard, J.L. Merz, P.M. Petroff, Phys. Rev. B 52 (1995) 5752.
[2] P. Paki, R. Leonelli, L. Isnard, R.A. Masut, J. Appl. Phys. 86 (1999) 6789.
[3] S. Hinooda, S. Loualiche, B. Lambert, N. Bertu, M. Paillard, X. Marie, T. Amand, Appl. Phys. Lett. 78 (2001) 3052.
[4] P.W. Fry, I.E. Itskevich, S.R. Parnell, J.J. Finley, L.R. Wilson, K.L. Schumacher, D.J. Mowbray, M.S. Skolnick, M. Al-Khafaji, A.G. Cullis, M. Hopkinson, J.C. Clark, G. Hill, Phys. Rev. B 62 (2000) 16784.
[5] F.H. Pollak, in: M. Balkanski (Ed.), Handbook on Semiconductors, North-Holland, New York, 1994.
[6] C.M. Lai, F.Y. Chang, C.W. Chang, C.H. Kao, H.H. Lin, G.J. Jan, J. Lee, Appl. Phys. Lett. 82 (2003) 3895.
[7] N.H. Bonadeo, A.S. Lenihan, G. Chen, J.R. Guest, D. Gammon, D.S. Katzer, D. Park, Appl. Phys. Lett. 75 (1999) 2933.
[8] H. Shen, M. Dutta, J. Appl. Phys. 78 (1995) 2151.

[9] M. Gendry, C. Monat, J. Brault, P. Regreny, G. Hollinger, B. Salem, G. Guillot, T. Benyattou, C. Bru-chevallier, G. Bremond, J. Appl. Phys. 95 (2004) 4761.

[10] B. Salem, T. Benyattou, G. Guillot, C. Bru-Chevallier, G. Bremond, C. Monat, G. Hollinger, M. Gendry, Phys. Rev. B 66 (2002) 193305.

[11] H. Lipsanen, M. Sopanen, J. Ahopelto, Phys. Rev. B 51 (13868) (1995) 13868.

[12] P. Miska, J. Even, C. Platz, B. Salem, T. Benyattou, C. Bru-Chevallier, G. Guillot, G. Bremond, Kh. Moumanis, F.H. Julien, O. Marty, C. Monat, M. Gendry, J. Appl. Phys. 95 (2004) 1074.

[13] R. Heitz, O. Stier, I. Mukhamezhanov, A. Madhukar, D. Bimberg, Phys. Rev. B 62 (2000) 11017.

[14] B.V. Shanabrook, O.J. Glembocki, W.T. Beard, Phys. Rev. B 35 (1986) 2540.

[15] P. Lautenschlager, M. Garriga, S. Logothetidis, M. Cardona, Phys. Rev. B 35 (1987) 9174.

[16] G.L. Rowland, T.J.C. Hosea, S. Malik, D. Childs, R. Murray, Appl. Phys. Lett. 73 (1998) 3268.

[17] W.-H. Chang, H.-Y. Chen, H.-S. Chang, W.-Y. Chen, T.M. Hsu, T.-P. Hsieh, J.-I. Chyi, N.-T. Yeh, Appl. Phys. Lett. 86 (2005) 131917.

[18] V. Davydov, I. Ignatiev, H.-W. Ren, S. Sugou, Y. Masumoto, Appl. Phys. Lett. 74 (1999) 3002.

[19] B. Salem, J. Olivares, G. Guillot, G. Bremond, J. Brault, C. Monat, M. Gendry, G. Hollinger, F. Hassen, H. Maaref, Appl. Phys. Lett. 79 (2001) 4435.